ELASTODYNAMICKÁ ANALÝZA PLOCHÝCH ORTOTRÓPNYCH ŠKRUPÍN

ELASTODYNAMIC ANALYSIS OF ORTHOTROPIC SHALLOW SHELLS

Ján SLADEK, Vladimír SLADEK[1]

Abstrakt

Bezprvková lokálna Petrov-Galerkinova formulácia je použitá pre analýzu plochých škrupín s ortotropickými materiálovými vlastnosťami. Reissnerova teória je použitá pre popis deformácie škrupín. Uvažuje sa statické ale aj dynamické zaťaženie. Pri riešení nestacionárneho dynamického zaťaženia sa využíva Laplaceova transformácia na elimináciu časovej premennej v riadiacich rovniciach. Slabá formulácia riadiacich rovníc so skokovou jednotkovou testovacou funkciou vedie k odvodeniu lokálnych integrálnych rovníc na podoblastiach pokrývajúcich povrch základnej roviny škrupiny. Podoblasti majú jednoduchý kruhový tvar a ich stredy sú uzlovými bodmi rozmiestnenými na analyzovanej oblasti škrupiny. Pohyblivá metóda najmenších štvorcov sa využíva na bezprvkovú aproximáciu fyzikálnych veličín. Neznáme Laplaceove obrazy veličín sa vypočítajú z lokálnych integrálnych rovníc. Časová závislosť sa získa po inverznej Laplaceovej transformacii pomocou Stehfest inverznej techniky.

Kľúčové slová: Reissnerova teória, lokálne integrálne rovnice, Laplaceova transformácia, Stehfestova inverzia, MLS aproximácia, statické a dynamické zaťaženie.

Abstract

A meshless local Petrov-Galerkin (MLPG) formulation is presented for bending problems of shear deformable shallow shells with orthotropic material properties. Shear deformation of shells described by the Reissner theory is considered. Analyses of shells under static and dynamic loads are given here. For transient elastodynamic case the Laplace-transform is used to eliminate the time dependence of the field variables. A weak formulation with a unit test function transforms the set of governing equations into local integral equations on local subdomains in the plane domain of the shell. Nodal points are randomly spread in that domain and each node is surrounded by a circular subdomain to which local integral equations are applied. The meshless approximation based on the Moving Least-Squares (MLS) method is employed for the implementation. Unknown Laplace-transformed quantities are computed from the local boundary integral equations. The time-dependent values are obtained by the Stehfest's inversion technique.

Keywords: Reissner theory, local boundary integral equations, Laplace-transform, Stehfest's inversion, MLS approximation, static and impact loads.

[1] prof. Ing. Ján SLADEK, DrSc., prof. RNDr. Vladimír SLADEK, DrSc., Institute of Construction and Architecture, Slovak Academy of Sciences, Bratislava jan.sladek@savba.sk, vladimir.sladek@savba.sk
Lektoroval: Dr.h.c. prof. Ing. František TREBUŇA, CSc., KAMaM, SjF TU v Košiciach, frantisek.trebuna@tuke.sk

INTRODUCTION

In recent years the demand for construction of huge and lightweight shell and spatial structures has been increasing. For the last three decades, some numerical methods such as Finite Difference Method (FDM) and Finite Element Method (FEM) have been successfully developed to solve the problems. Boundary Element Method (BEM) has emerged as an alternative numerical method to solve plate and shell problems. Review article devoted to early applications of BEM to shells is given by Beskos (1991). The first application of BEM to shells is given by Newton and Tottenham (1968), where they presented a method based on the decomposition of the fourth-order governing equation into a set of the second-order ones. Tosaka and Miyake (1983) developed a direct BEM formulation for shallow shells. Lu and Huang (1992) derived a direct BEM formulation for shallow shells involving shear deformation. For elastodynamic shell problems it is appropriate to use the weighted residual method with static fundamental solution as a test function [Zhang and Atluri (1986), Providakis and Beskos (1991)]. All previous BEM applications are dealing with isotropic shallow shells. Only Wang and Schweizerhof (1996a-b) applied boundary integral equation method for moderately thick laminated orthotropic shallow shells. They used the static fundamental solution corresponding to a shear deformable orthotropic shell and applied it for study of free vibration of thick shallow shells. The fundamental solution for a thick orthotropic shell under a dynamic load is not available according the best of author's knowledge.

Meshless approaches for problems of continuum mechanics have attracted much attention during the past decade [Belytschko et al. (1994), Atluri (2004)]. In spite of the great success of the FEM and the BEM as accurate and effective numerical tools for the solution of boundary value problems with complex domains, there is still a growing interest in developing new advanced numerical methods. In recent years, meshfree or meshless formulations are becoming to be popular due to their high adaptivity and low costs to prepare input data for numerical analyses. In methods based on local weak-form formulation no cells are required and therefore they are often referred to as truly meshless methods. If a simple form is chosen for the geometry of the subdomains, numerical integrations can be easily carried out over them. The meshless local Petrov-Galerkin (MLPG) method is a fundamental base for the derivation of many meshless formulations, since the trial and test functions can be chosen from different functional spaces. The method has been successfully applied to plate problems [Sladek et al. (2003)].

The first application of a meshless method to shell problems was given by Krysl and Belytschko (1996), where they applied the element-free Galerkin method. The moving least-square approximation yields C^1 continuity which satisfies the Kirchhoff hypothesis. Their results showed excellent convergence, however, their formulation is not applicable to shear deformable plate/shell problems. Recently, Noguchi et al. (2000) used a mapping technique to transform the curved surface into flat two-dimensional space. Then, the element-free Galerkin method can be applied also to thick plates or shells including the shear deformation effects.

In the present paper, the authors have developed for the first time a meshless method based on the local Petrov-Galerkin weak-form to solve dynamic problems for orthotropic thick shallow shells. The Reissner theory reduces the original 3-d thick shell problem to a 2-d problem. Nodal points are randomly spread in that domain and each node is surrounded by a circular subdomain to which local integral equations are applied. The Laplace-transform technique is applied to the set of governing differential equations for elastodynamic Reissner shell bending theory. A unit test function is used in the local weak-form of the governing equations for transformed fields. The meshless approximation based on the Moving Least-Squares (MLS) method is employed for the implementation. The Stehfest's inversion method [Stehfest (1970)] is employed to obtain the time-dependent solution.

LOCAL INTEGRAL EQUATIONS FOR SHEAR DEFORMABLE SHELLS

Consider an elastic orthotropic shallow shell of the constant thickness *h* and with its mid surface being described by $x_3 = f(x_1, x_2)$ in a domain Ω with the boundary contour Γ in the base plane $x_1 - x_2$. The shell is subjected to a transient dynamic load $q_i(\mathbf{x}, t)$. Using the Reissner`s linear theory of shallow shells [Reissner (1946)], the equilibrium equations may be written as

$$
\begin{aligned}
&M_{\alpha\beta,\beta}(\mathbf{x},t) - Q_\alpha(\mathbf{x},t) = \frac{\rho h^3}{12}\ddot{w}_\alpha(\mathbf{x},t) \ , \\
&Q_{\alpha,\alpha}(\mathbf{x},t) - k_{\alpha\beta}N_{\alpha\beta}(\mathbf{x},t) + q(\mathbf{x},t) = \rho h\ddot{w}_3(\mathbf{x},t) \\
&N_{\alpha\beta,\beta}(\mathbf{x},t) + q_\alpha(\mathbf{x},t) = \rho\ddot{u}_\alpha(\mathbf{x},t) \qquad \mathbf{x} \in \Omega \ ,
\end{aligned} \tag{1}
$$

where ρ is the mass density, w_3 represent the out-of-plane deflection, while u_α and w_α denote the in-plane displacements and the rotation in the x_α -direction, respectively, $M_{\alpha\beta}$ represent the bending moments, $N_{\alpha\beta}$ are normal force stress, and Q_α are the shear forces. Latin indices vary from 1 to 3 and Greek indices vary from 1 to 2. The dots indicate differentiations with respect to time *t*. The principal curvatures of the shell in x_1 and x_2 are denoted by k_{11} and k_{22}, respectively and $k_{12} = k_{21} = 0$.

The bending moments $M_{\alpha\beta}$, the shear forces Q_α and normal force stress $N_{\alpha\beta}$ are expressed in terms of the rotations and the lateral displacement for an orthotropic shell as [Lukasiewicz, 1979]

$$
\begin{aligned}
&M_{\alpha\beta} = D_{\alpha\beta}\left(w_{\alpha,\beta} + w_{\beta,\alpha}\right) + C_{\alpha\beta}w_{\gamma,\gamma} \\
&Q_\alpha = C_\alpha\left(w_\alpha + w_{3,\alpha}\right), \\
&N_{\alpha\beta} = P_{\alpha\beta}\left(u_{\alpha,\beta} + u_{\beta,\alpha}\right) + 2P_{\alpha\beta}k_{\alpha\beta}w_3 + Q_{\alpha\beta}(u_{\gamma,\gamma} + k_{\alpha\beta}w_3)
\end{aligned} \tag{2}
$$

where no summation is assumed in eq. (2) with respect to the indices α , β and the material parameters are given as

$$
\begin{aligned}
&D_{11} = \frac{D_1}{2}\left(1 - \nu_{21}\right) , \quad D_{22} = \frac{D_2}{2}\left(1 - \nu_{12}\right) , \quad D_{12} = D_{21} = D_k = \frac{G_{12}h^3}{12} , \\
&C_{11} = D_1\nu_{21} , \quad C_{22} = D_2\nu_{12} , \quad C_{12} = C_{21} = 0 , \\
&D_1 = \frac{E_1h^3}{12(1 - \nu_{12}\nu_{21})} , \quad D_2 = \frac{E_2h^3}{12(1 - \nu_{12}\nu_{21})} , \quad D_1\nu_{21} = D_2\nu_{12} , \\
&C_1 = G_{13}\kappa h , \quad C_2 = G_{23}\kappa h , \\
&P_{11} = \frac{P_1}{2}\left(1 - \nu_{21}\right) , \quad P_{22} = \frac{P_2}{2}\left(1 - \nu_{12}\right) , \quad P_{12} = P_{21} = G_{12}h ,
\end{aligned}
$$

$$P_1 = \frac{E_1 h}{(1-\nu_{12}\nu_{21})} \quad , \quad P_2 = \frac{E_2 h}{(1-\nu_{12}\nu_{21})} \quad , \quad Q_{11} = P_1\nu_{21} \ , \quad Q_{22} = P_2\nu_{12} \ ,$$
$$Q_{12} = Q_{21} = 0 \, ,$$

in which $\kappa = 5/6$ in the Reissner theory, E_1 and E_2 represent Young's moduli, G_{12}, G_{13} and G_{23} are shear moduli, ν_{12} and ν_{21} are Poisson's ratios, respectively.

To eliminate the time variable *t* in the governing equations (1), the Laplace-transform is applied to that system. Then, one can write

$$\bar{M}_{\alpha\beta,\beta}(\mathbf{x},s) - \bar{Q}_\alpha(\mathbf{x},s) = \frac{\rho h^3}{12} s^2 \bar{w}_\alpha(\mathbf{x},s) - \bar{R}_\alpha(\mathbf{x},s) \tag{3}$$

$$\bar{Q}_{\alpha,\alpha}(\mathbf{x},s) - k_{\alpha\beta}\bar{N}_{\alpha\beta}(\mathbf{x},s) = \rho h s^2 \bar{w}_3(\mathbf{x},s) - \bar{R}_3(\mathbf{x},s) \, , \tag{4}$$

$$\bar{N}_{\alpha\beta,\beta}(\mathbf{x},s) = \rho s^2 \bar{u}_\alpha(\mathbf{x},s) - \bar{R}'_\alpha(\mathbf{x},s) \, , \tag{5}$$

where *s* is the Laplace-transform parameter, and, $\bar{R}_\alpha$, $\bar{R}_3$ and $\bar{R}'_\alpha$ are given by

$$\bar{R}_\alpha(\mathbf{x},s) = \frac{\rho h^3}{12}\left[s w_\alpha(\mathbf{x}) + \dot{w}_\alpha(\mathbf{x}) \right] ,$$
$$\bar{R}_3(\mathbf{x},s) = \bar{q}(\mathbf{x},s) + \rho h s w_3(\mathbf{x}) + \rho h \dot{w}_3(\mathbf{x}) \ ,$$
$$\bar{R}'_\alpha(\mathbf{x},s) = \bar{q}_\alpha(\mathbf{x},s) + \rho s u_\alpha(\mathbf{x}) + \rho \dot{u}_\alpha(\mathbf{x}) \ ,$$

with $w_k(\mathbf{x})$, $u_\alpha(\mathbf{x})$ and $\dot{w}_k(\mathbf{x})$, $\dot{u}_\alpha(\mathbf{x})$ representing the initial values of bending and membrane displacements and their respective velocities.

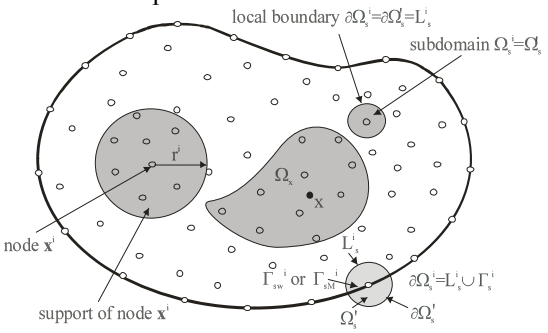

Fig.1 Local boundaries for weak formulation, the domain Ω_x for MLS approximation of the trial function, and support area of weight function around node $\mathbf{x}^i$

Instead of writing the global weak-form for the above governing equations, the MLPG methods construct the weak-form over local subdomains such as Ω_s , which is a small region taken for each node inside the global domain [Atluri (2004)]. The local subdomains overlap each other and cover the whole global domain Ω (Fig. 1). The local subdomains could be of any geometrical shape and size. In the current paper, the local subdomains are taken to be of circular shape. The local weak-form of the governing equations (3), (4) and (5) for $\mathbf{x}^i \in \Omega_s^i$ can be written as

$$\int_{\Omega_s^i}\left[\bar{M}_{\alpha\beta,\beta}(\mathbf{x},s)-\bar{Q}_\alpha(\mathbf{x},s)-\frac{\rho h^3}{12}s^2\bar{w}_\alpha(\mathbf{x},s)+\bar{R}_\alpha(\mathbf{x},s)\right]w^*_{\alpha\gamma}(\mathbf{x})d\Omega=0\ , \tag{6}$$

$$\int_{\Omega_s^i}\left[\bar{Q}_{\alpha,\alpha}(\mathbf{x},s)-k_{\alpha\beta}\bar{N}_{\alpha\beta}(\mathbf{x},s)-\rho hs^2\bar{w}_3(\mathbf{x},s)+\bar{R}_3(\mathbf{x},s)\right]w^*(\mathbf{x})d\Omega=0\ , \tag{7}$$

$$\int_{\Omega_s^i}\left[\bar{N}_{\alpha\beta,\beta}(\mathbf{x},s)-\rho s^2\bar{u}_\alpha(\mathbf{x},s)+\bar{R}'_\alpha(\mathbf{x},s)\right]u^*_{\alpha\gamma}(\mathbf{x})d\Omega=0\ , \tag{8}$$

where $w^*_{\alpha\beta}(\mathbf{x})$, $u^*_{\alpha\beta}(\mathbf{x})$ and $w^*(\mathbf{x})$ are weight (test) functions.

Applying the Gauss divergence theorem to eqs. (6) - (8) one obtains

$$\int_{\partial\Omega_s^i}\bar{M}_\alpha(\mathbf{x},s)w^*_{\alpha\gamma}(\mathbf{x})d\Gamma-\int_{\Omega_s^i}\left[\bar{M}_{\alpha\beta}(\mathbf{x},s)w^*_{\alpha\gamma,\beta}(\mathbf{x})+\bar{Q}_\alpha(\mathbf{x},s)w^*_{\alpha\gamma}(\mathbf{x})\right]d\Omega-$$

$$-\int_{\Omega_s^i}\left(\frac{\rho h^3}{12}s^2\bar{w}_\alpha(\mathbf{x},s)-\bar{R}_\alpha(\mathbf{x},s)\right)w^*_{\alpha\gamma}(\mathbf{x})d\Omega=0\ , \tag{9}$$

$$\int_{\partial\Omega_s^i}\bar{Q}_\alpha(\mathbf{x},s)n_\alpha(\mathbf{x})w^*(\mathbf{x})d\Gamma-\int_{\Omega_s^i}\left[\bar{Q}_\alpha(\mathbf{x},s)w^*_{,\alpha}(\mathbf{x})+k_{\alpha\beta}(\mathbf{x})\bar{N}_{\alpha\beta}(\mathbf{x},s)w^*(\mathbf{x})\right]d\Omega-$$

$$-\int_{\Omega_s^i}\left(\rho hs^2\bar{w}_3(\mathbf{x},s)-\bar{R}_3(\mathbf{x},s)\right)w^*(\mathbf{x})d\Omega=0\ , \tag{10}$$

$$\int_{\partial\Omega_s^i}\bar{T}_\alpha(\mathbf{x},s)u^*_{\alpha\gamma}(\mathbf{x})d\Gamma-\int_{\Omega_s^i}\left[\bar{N}_{\alpha\beta}(\mathbf{x},s)u^*_{\alpha\gamma,\beta}(\mathbf{x})+\left(\rho s^2\bar{u}_\alpha(\mathbf{x},s)-\bar{R}'_\alpha(\mathbf{x},s)\right)u^*_{\alpha\gamma}(\mathbf{x})\right]d\Omega=0 \tag{11}$$

where $\partial\Omega_s^i$ is the boundary of the local subdomain and

$$\bar{M}_\alpha(\mathbf{x},s)=\bar{M}_{\alpha\beta}(\mathbf{x},s)n_\beta(\mathbf{x})\ ,\ \bar{T}_\alpha(\mathbf{x},s)=\bar{N}_{\alpha\beta}(\mathbf{x},s)n_\beta(\mathbf{x}) \tag{12}$$

are the Laplace-transforms of the normal bending moments and traction vector, and n_α is the outward unit normal vector to the boundary. The local weak-forms (9) - (11) are the starting point for derivation of local boundary-domain integral equations with choosing appropriate test functions. The test functions $w^*_{\alpha\beta}(\mathbf{x})$, $u^*_{\alpha\beta}(\mathbf{x})$ and $w^*(\mathbf{x})$ can be taken to correspond to a unit step function in each subdomain, i.e.

$$w^*_{\alpha\gamma}(\mathbf{x})=u^*_{\alpha\gamma}(\mathbf{x})=\begin{cases}\delta_{\alpha\gamma} & \text{at } \mathbf{x}\in\left(\Omega_s\cup\partial\Omega_s\right)\\ 0 & \text{at } \mathbf{x}\notin\left(\Omega_s\cup\partial\Omega_s\right)\end{cases}\ ,$$

$$u^*(\mathbf{x})=\begin{cases}1 & \text{at } \mathbf{x}\in\left(\Omega_s\cup\partial\Omega_s\right)\\ 0 & \text{at } \mathbf{x}\notin\left(\Omega_s\cup\partial\Omega_s\right)\end{cases}\ . \tag{13}$$

Then, the local weak-forms (9) - (11) are transformed into simple local boundary-domain integral equations

$$\int_{\partial\Omega_s^i}\bar{M}_\alpha(\mathbf{x},s)d\Gamma-\int_{\Omega_s^i}\bar{Q}_\alpha(\mathbf{x},s)d\Omega-\int_{\Omega_s^i}\frac{\rho h^3}{12}s^2\bar{w}_\alpha(\mathbf{x},s)d\Omega+\int_{\Omega_s^i}\bar{R}_\alpha(\mathbf{x},s)d\Omega=0 \tag{14}$$

$$\int_{\partial\Omega_s^i} \bar{Q}_\alpha(\mathbf{x},s)n_\alpha(\mathbf{x})d\Gamma - \int_{\Omega_s^i} k_{\alpha\beta}(\mathbf{x})\bar{N}_{\alpha\beta}(\mathbf{x},s)d\Omega - \int_{\Omega_s^i} \rho h s^2 \bar{w}_3(\mathbf{x},s)d\Omega + \int_{\Omega_s^i} \bar{R}_3(\mathbf{x},s)d\Omega = 0 \tag{15}$$

$$\int_{\partial\Omega_s^i} \bar{T}_\alpha(\mathbf{x},s)d\Gamma - \int_{\Omega_s^i} \rho s^2 \bar{u}_\alpha(\mathbf{x},s)d\Omega + \int_{\Omega_s^i} \bar{R}'_\alpha(\mathbf{x},s)d\Omega = 0\,. \tag{16}$$

In the MLPG method the test and the trial functions are not necessarily from the same functional spaces. The trial function is chosen to be the moving least-squares (MLS) interpolation over a number of nodes randomly spread within the domain of influence. Without going into detail the Laplace transform of deflection and rotations can be approximated [Sladek et al. (2006)] by

$$\bar{\mathbf{w}}^h(\mathbf{x},s) = \mathbf{\Phi}^T(\mathbf{x})\cdot\hat{\mathbf{w}}(s) = \sum_{a=1}^{n} \phi^a(\mathbf{x})\hat{\mathbf{w}}^a(s) \quad , \tag{17}$$

where

$$\mathbf{\Phi}^T(\mathbf{x}) = \mathbf{p}^T(\mathbf{x})\mathbf{A}^{-1}(\mathbf{x})\mathbf{B}(\mathbf{x}) \ . \tag{18}$$

Similarly, one can obtain the approximation for the in-plane displacements

$$\bar{\mathbf{u}}^h(\mathbf{x},s) = \mathbf{\Phi}^T(\mathbf{x})\cdot\hat{\mathbf{u}}(s) = \sum_{a=1}^{n} \phi^a(\mathbf{x})\hat{\mathbf{u}}^a(s) \quad . \tag{19}$$

In eq. (17), $\phi^a(\mathbf{x})$ is usually referred to as the shape function of the MLS approximation corresponding to the nodal point $\mathbf{x}^a$. Matrices **A** and **B** and monomial polynom $p(\mathbf{x})$ are defined in [Sladek et al. (2006)].

The partial derivatives of the MLS shape functions are obtained as [Atluri (2004)]

$$\phi^a{}_{,k} = \sum_{j=1}^{m}\left[p^j{}_{,k}(\mathbf{A}^{-1}\mathbf{B})^{ja} + p^j(\mathbf{A}^{-1}\mathbf{B}_{,k} + \mathbf{A}^{-1}_{,k}\mathbf{B})^{ja}\right] \tag{20}$$

wherein $\mathbf{A}^{-1}_{,k} = \left(\mathbf{A}^{-1}\right)_{,k}$ represents the derivative of the inverse of **A** with respect to x_k , which is given by

$$\mathbf{A}^{-1}_{,k} = -\mathbf{A}^{-1}\mathbf{A}_{,k}\mathbf{A}^{-1} \ .$$

The directional derivatives of $\bar{\mathbf{w}}(\mathbf{x},s)$ and $\bar{\mathbf{u}}(\mathbf{x},s)$ are approximated in terms of the same nodal values as the primary fields by

$$\bar{\mathbf{w}}_{,k}(\mathbf{x},s) = \sum_{a=1}^{n} \hat{\mathbf{w}}^a(s)\phi^a_{,k}(\mathbf{x}) \tag{21}$$

$$\bar{\mathbf{u}}_{,k}(\mathbf{x},s) = \sum_{a=1}^{n} \hat{\mathbf{u}}^a(s)\phi^a_{,k}(\mathbf{x}) \tag{22}$$

Substituting approximation (21) into the definition for the normal bending moments (12) $\left[\bar{M}_1(\mathbf{x},s),\ \bar{M}_2(\mathbf{x},s)\right]^T$ and using Eq. (2), one obtains

$$\bar{\mathbf{M}}(\mathbf{x},s) = \mathbf{N_1}\sum_{a=1}^{n}\mathbf{B}_1^a(\mathbf{x})\mathbf{w}^{*a}(s) \ + \mathbf{N_2}\sum_{a=1}^{n}\mathbf{B}_2^a(\mathbf{x})\mathbf{w}^{*a}(s) \ = \mathbf{N}_\alpha(\mathbf{x})\sum_{a=1}^{n}\mathbf{B}_\alpha^a(\mathbf{x})\mathbf{w}^{*a}(s) \quad , \tag{23}$$

where the vector $\mathbf{w}^{*a}(s)$ is defined as a column vector $\mathbf{w}^{*a}(s)=\left[\hat{w}_1^a(s),\ \hat{w}_2^a(s)\right]^T$, the matrices $\mathbf{N}_\alpha(\mathbf{x})$ are related to the normal vector **n(x)** on $\partial\Omega_S$ by

$$\mathbf{N}_1(\mathbf{x})=\begin{bmatrix} n_1 & 0 & n_2 \\ 0 & n_2 & n_1 \end{bmatrix} \quad \text{and} \quad , \quad \mathbf{N}_2(\mathbf{x})=\begin{bmatrix} C_{11} & 0 \\ 0 & C_{22} \end{bmatrix}\begin{bmatrix} n_1 & n_1 \\ n_2 & n_2 \end{bmatrix}$$

and the matrices $\mathbf{B}_\alpha^a$ are represented by the gradients of the shape functions as

$$\mathbf{B}_1^a(\mathbf{x})=\begin{bmatrix} 2D_{11}\phi_{,1}^a & 0 \\ 0 & 2D_{22}\phi_{,2}^a \\ D_{12}\phi_{,2}^a & D_{12}\phi_{,1}^a \end{bmatrix} \quad , \quad \mathbf{B}_2^a(\mathbf{x})=\begin{bmatrix} \phi_{,1}^a & 0 \\ 0 & \phi_{,2}^a \end{bmatrix}.$$

Similarly one can obtain the approximation for the shear forces

$$\bar{\mathbf{Q}}(\mathbf{x},s)=\mathbf{C}(\mathbf{x})\sum_{a=1}^{n}\left[\phi^a(\mathbf{x})\mathbf{w}^{*a}(s)+\mathbf{F}^a(\mathbf{x})\hat{w}_3^a(s)\right],$$

where $\bar{\mathbf{Q}}(\mathbf{x},s)=\left[\bar{Q}_1(\mathbf{x},s),\ \bar{Q}_2(\mathbf{x},s)\right]^T$ and

$$\mathbf{C}(\mathbf{x})=\begin{bmatrix} C_1(\mathbf{x}) & 0 \\ 0 & C_2(\mathbf{x}) \end{bmatrix}, \quad \mathbf{F}^a(\mathbf{x})=\begin{bmatrix} \phi_{,1}^a \\ \phi_{,2}^a \end{bmatrix} \quad ,$$

and the traction vector $\left[\bar{P}_1(\mathbf{x},s),\ \bar{P}_2(\mathbf{x},s)\right]^T$ defined by eq. (12)

$$\bar{\mathbf{P}}(\mathbf{x},s)=\mathbf{N}_1(\mathbf{x})\sum_{a=1}^{n}\mathbf{H}_1^a(\mathbf{x})\mathbf{u}^{*a}(s) \ +\mathbf{N}_2'(\mathbf{x})\sum_{a=1}^{n}\mathbf{B}_2^a(\mathbf{x})\mathbf{u}^{*a}(s) \ +\mathbf{G}(\mathbf{x})\sum_{a=1}^{n}\phi^a(\mathbf{x})\hat{w}_3^a(s) \ =$$

$$=\mathbf{N}_\alpha'(\mathbf{x})\sum_{a=1}^{n}\mathbf{H}_\alpha^a(\mathbf{x})\mathbf{u}^{*a}(s) \ +\mathbf{G}(\mathbf{x})\sum_{a=1}^{n}\phi^a(\mathbf{x})\hat{w}_3^a(s) \ , \tag{24}$$

where the vector $\mathbf{u}^{*a}(s)$ is defined as a column vector $\mathbf{u}^{*a}(s)=\left[\hat{u}_1^a(s),\ \hat{u}_2^a(s)\right]^{\mathrm{T}}$,

$$\mathbf{H}_1^a(\mathbf{x})=\begin{bmatrix} 2P_{11}\phi_{,1}^a & 0 \\ 0 & 2P_{22}\phi_{,2}^a \\ P_{12}\phi_{,2}^a & P_{12}\phi_{,1}^a \end{bmatrix} \quad , \quad \mathbf{N}_2'(\mathbf{x})=\begin{bmatrix} Q_{11} & 0 \\ 0 & Q_{22} \end{bmatrix}\begin{bmatrix} n_1 & n_1 \\ n_2 & n_2 \end{bmatrix} ,$$

$$\mathbf{N}_1'(\mathbf{x})=\mathbf{N}_1(\mathbf{x}) \quad , \quad \mathbf{H}_2^a(\mathbf{x})=\mathbf{B}_2^a(\mathbf{x}) ,$$

and $\mathbf{G}(\mathbf{x})$ is given by

$$\mathbf{G}(\mathbf{x})=\begin{bmatrix} k_{11}(2P_{11}+Q_{11})n_1 \\ k_{22}(2P_{22}+Q_{22})n_2 \end{bmatrix}.$$

We need to approximate also

$$k_{\alpha\beta}(\mathbf{x})\bar{N}_{\alpha\beta}(\mathbf{x},s)=\sum_{a=1}^{n}\mathbf{K}^a(\mathbf{x})^{\mathrm{T}}\mathbf{u}^{*a}(s) \ +O(\mathbf{x})\sum_{a=1}^{n}\phi^a(\mathbf{x})\hat{w}_3^a(s) \quad , \tag{25}$$

where $\mathbf{K}^a(\mathbf{x}) = \begin{bmatrix} (2P_{11}+Q_{11})k_{11}\phi^a_{,1} + Q_{22}k_{22}\phi^a_{,1} \\ (2P_{22}+Q_{22})k_{22}\phi^a_{,2} + Q_{11}k_{11}\phi^a_{,2} \end{bmatrix}$

$$O(\mathbf{x}) = \left[(2P_{11}+Q_{11})k_{11}(\mathbf{x})k_{11}(\mathbf{x}) + (2P_{22}+Q_{22})k_{22}(\mathbf{x})k_{22}(\mathbf{x})\right] .$$

Furthermore, in view of the MLS-approximations (23) and (25) for the unknown fields in the local boundary integral equations (14) - (16), we obtain the discretized LIEs

$$\sum_{a=1}^{n}\left[\int_{L_s^i+\Gamma_{sw}^i}\mathbf{N}_\alpha(\mathbf{x})\mathbf{B}_\alpha^a(\mathbf{x})d\Gamma - \int_{\Omega_s^i}\left(\mathbf{C}(\mathbf{x}) + \mathbf{E}\frac{\rho h^3(\mathbf{x})}{12}s^2\right)\phi^a(\mathbf{x})d\Omega\right]\mathbf{w}^{*a}(s) -$$

$$-\sum_{a=1}^{n}\hat{w}_3^a(s)\int_{\Omega_s^i}\mathbf{C}(\mathbf{x})\mathbf{F}^a(\mathbf{x})d\Omega = -\int_{\Gamma_{sM}^i}\tilde{\tilde{\mathbf{M}}}(\mathbf{x},s)d\Gamma - \int_{\Omega_s^i}\bar{\mathbf{R}}(\mathbf{x},s)d\Omega , \tag{26}$$

$$\sum_{a=1}^{n}\left(\int_{\partial\Omega_s^i}\mathbf{C}_n(\mathbf{x})\phi^a(\mathbf{x})d\Gamma\right)\mathbf{w}^{*a}(s) - \sum_{a=1}^{n}\left[\int_{\Omega_s^i}\mathbf{K}^a(\mathbf{x})^{\mathrm{T}}d\Omega\right]\mathbf{u}^{*a}(s) +$$

$$+\sum_{a=1}^{n}\hat{w}_3^a(s)\left(\int_{\partial\Omega_s^i}\mathbf{C}_n(\mathbf{x})\mathbf{F}^a(\mathbf{x})d\Gamma - \int_{\Omega_s^i}O(\mathbf{x})\phi^a(\mathbf{x})d\Omega - \rho h s^2\int_{\Omega_s^i}\phi^a(\mathbf{x})d\Omega\right) =$$

$$= -\int_{\Omega_s^i}\bar{R}_3(\mathbf{x},s)d\Omega , \tag{27}$$

$$\sum_{a=1}^{n}\left[\int_{L_s^i+\Gamma_{su}^i}\mathbf{N}'_\alpha(\mathbf{x})\mathbf{H}_\alpha^a(\mathbf{x})d\Gamma - \rho s^2\mathbf{E}\int_{\Omega_s^i}\phi^a(\mathbf{x})d\Omega\right]\mathbf{u}^{*a}(s) + \sum_{a=1}^{n}\hat{w}_3^a(s)\int_{\Omega_s^i}\mathbf{G}(\mathbf{x})\phi^a(\mathbf{x})d\Omega =$$

$$= -\int_{\Gamma_{sP}^i}\tilde{\tilde{\mathbf{T}}}(\mathbf{x},s)d\Gamma - \int_{\Omega_s^i}\bar{\mathbf{R}}'(\mathbf{x},s)d\Omega \tag{28}$$

in which

$$\mathbf{E} = \begin{pmatrix} 1 & 0 \\ 0 & 1 \end{pmatrix}, \quad \mathbf{C}_n(\mathbf{x}) = \begin{pmatrix} n_1, & n_2 \end{pmatrix}\begin{pmatrix} C_1 & 0 \\ 0 & C_2 \end{pmatrix} = \begin{pmatrix} C_1 n_1, & C_2 n_2 \end{pmatrix}.$$

Recall that the LIE (26)-(28) are considered on the sub-domains adjacent to the interior nodes $\mathbf{x}^i$ as well as to the boundary nodes on Γ_{sM}^i and Γ_{sP}^i. For the source point $\mathbf{x}^i$ located on the global boundary Γ the boundary of the subdomain $\partial\Omega_s^i$ is composed of the interior and boundary portions L_s^i and Γ_{sM}^i, respectively, or alternatively of L_s^i and Γ_{sP}^i, with the portions Γ_{sM}^i and Γ_{sP}^i lying on the global boundary with prescribed bending moments or stress vector, respectively, as shown in Fig. 1. The LIEs (26) and (28) are vector equations for two components of rotations and in-plane displacements, respectively. Then, set of LIEs (26)-(28) represents 5 equations in each node for five unknown components, two rotations, deflection and two in-plane displacements.

It should be noted here that there are neither Lagrange-multipliers nor penalty parameters introduced into the local weak-forms (6) - (8) because the essential boundary conditions on Γ_{sw}^{i} or Γ_{su}^{i} can be imposed directly by using the interpolation approximations (17) and (19)

$$\sum_{a=1}^{n} \phi^{a}(\mathbf{x})\hat{\mathbf{w}}^{a}(s) = \tilde{\tilde{\mathbf{w}}}(\mathbf{x}^{i}, s) \quad \text{for} \quad \mathbf{x}^{i} \in \Gamma_{sw}^{i} \tag{29}$$

$$\sum_{a=1}^{n} \phi^{a}(\mathbf{x})\hat{\mathbf{u}}^{a}(s) = \tilde{\tilde{\mathbf{u}}}(\mathbf{x}^{i}, s) \quad \text{for} \quad \mathbf{x}^{i} \in \Gamma_{su}^{i} \ , \tag{30}$$

where $\tilde{\tilde{\mathbf{w}}}(\mathbf{x}^{i}, s)$ and $\tilde{\tilde{\mathbf{u}}}(\mathbf{x}^{i}, s)$ are the Laplace transforms of the generalized displacement vector prescribed on the boundary Γ_{sw}^{i} and Γ_{su}^{i}, respectively.

The time-dependent values of the transformed quantities in the previous consideration can be obtained by an inverse transformation. There are many inversion methods available for the inverse Laplace-transformation. As the inverse Laplace-transformation is an ill-posed problem, small truncation errors can be greatly magnified in the inversion process and hence lead to poor numerical results. In the present analysis, the sophisticated Stehfest's algorithm [Stehfest (1970)] for the numerical inversion is used.

NUMERICAL EXAMPLES

A clamped shallow spherical shell with square contour and orthotropic material properties is analyzed. The shell is subjected to a uniformly distributed impact load with Heaviside time variation. The following geometrical and material parameters are assumed: side length of the shell $a = 0.254\text{m}$, thickness $h = 0.0127\text{m}$, Young's moduli $E_2 = 0.6895 \cdot 10^{10}\ \text{N/m}^2$, $E_1 = 2E_2$, Poisson's ratios $\nu_{21} = 0.15$, $\nu_{12} = 0.3$ and mass density $\rho = 7.166 \times 10^{3}\ \text{kgm}^{-3}$. The used shear moduli correspond to Young's modulus E_2, namely, $G_{12} = G_{13} = G_{23} = E_2 / 2(1+\nu_{12})$.

In our numerical calculations, 441 nodes with a regular distribution were used for the approximation of the rotations and the deflection (Fig.2). The time variation of the central deflection of the shell with the curvature $R/a = 10$ is presented in Fig. 3. The time variable is normalized by $t_0 = a^2 / 4\sqrt{\rho h / D} = 1.35 \cdot 10^{-2} s$, corresponding to isotropic plate with $E_1 = E_2$. Deflections are normalized by $w_3^p(a/2) = 8.842 \cdot 10^{-3} m$ corresponding to plate deflection. For the FEM analysis we have used 400 quadrilateral eight-node shell elements with 1000 time increments. One can observe quite good agreement between both the MLPG and FEM results.

The influence of the shell curvature on the time variation of central deflection is presented in Fig. 4. For the deeper shell, the peak value of the deflection is reached at an earlier time instant than for the shallower shell. Similar to the static case, the maximum value of the deflection is lower for more curved shell. The time-variation of the central bending moment M_{11} of the clamped square shallow spherical shell with the curvature $R/a = 10$ is presented in Fig. 5. Small discrepancies of the present MLPG and FEM results are observed here mainly for larger instants. It can be caused by inaccuracy of the Laplace inversion technique. However, the

periodicity of the deflection oscillations and the maximal values are almost the same for both the results.

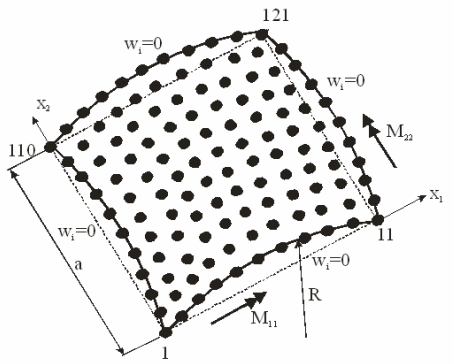

Fig.2 Geometry and boundary conditions used for the square shallow spherical shell

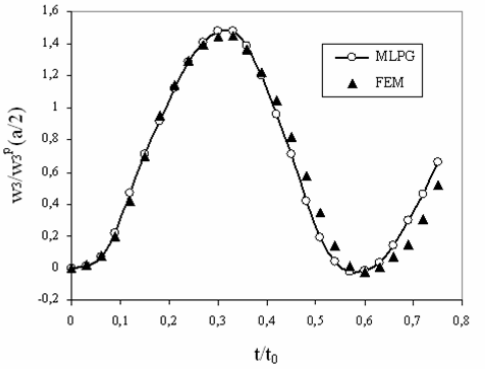

Fig.3 Time-variation of central deflection of clamped square shallow spherical shell with curvature $R / a = 10$ and subjected to a suddenly applied uniform load

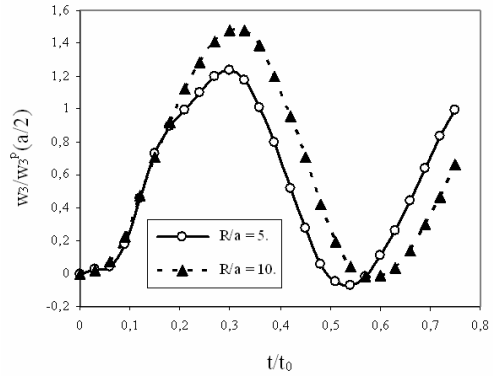

Fig.4 Influence of the shell curvatures on the time variation of central deflection of clamped square shallow spherical shell

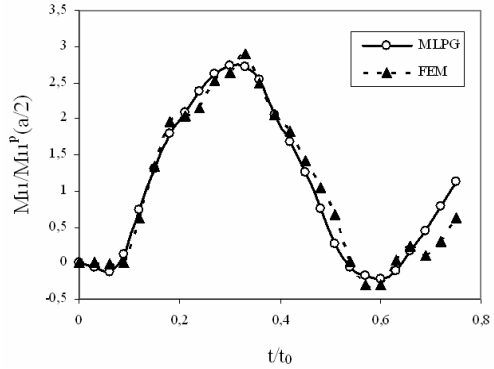

Fig.5 Time-variation of central bending moment M_{11} of clamped square shallow spherical shell with curvature $R / a = 10$ subjected to a suddenly applied uniform load

Now, the same square shallow shell as in the previous example with simply supported boundary conditions is analysed. Again the impact load with a Heaviside time variation is considered. The time-variation of the central deflections of simply supported square shallow spherical shell with curvatures $R / a = 10$ is presented in Fig. 6. A very good agreement of the present MLPG and FEM results is observed here.

The influence of the shell curvature on the time variation of central deflection is presented in Fig. 7. As in the case of clamped shell, one can observe higher frequency of the oscillations of deflections for the shell with higher curvature. Oppositely, the amplitude of the deflection is reduced for such a shell. A larger influence of the shell curvature on the amplitude of the deflection is observed here than in the case of clamped shell.

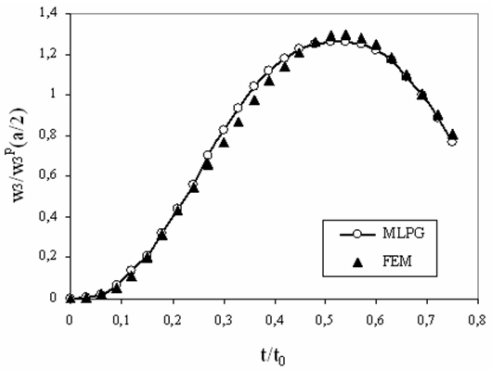

Fig.6 Time-variation of central deflection of simply supported square shallow spherical shell with curvature $R / a = 10$ and subjected to a suddenly applied uniform load

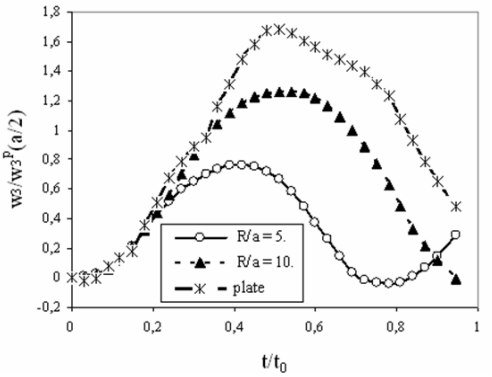

Fig.7 Influence of the shell curvatures on the time variation of central deflection of simply supported square shallow spherical shell

CONCLUSIONS

A meshless local Petrov-Galerkin method has been successfully applied to orthotropic shallow shells under static and dynamic load. The behaviour of shells is described by the Reissner theory. The Laplace-transform technique is applied to eliminate the time variable in the coupled governing differential equations of the Reissner theory. The use of the Laplace-transform in forced vibration analysis converts the dynamic problem to a set of quasi-static problems. The proposed method is an alternative to existing computational methods. Its main advantage is the simplicity. The present formulation possesses the generality of the FEM. Therefore, the method seems to be promising to analyze problems, which cannot be solved effectively by the conventional BEM.

The authors acknowledge the supports by the Slovak Research and Development Support Agency registered under the project number APVT-20-035404, by the Slovak Grant Agency under the project number VEGA – 2/6109/6.

REFERENCES

[1] ATLURI, S. N.: *The Meshless Method , (MLPG) For Domain & BIE Discretizations*, Tech Science Press, 2004

[2] BELYTSCHKO, T., KROGAUZ, Y., ORGAN, D., FLEMING, M., KRYSL, P.: *Meshless methods, an overview and recent developments*. Comp. Meth. Appl. Mech. Engn., 139, 1996, p. 3-47

[3] BESKOS D.E.: *Static and dynamic analysis of shells*, In Boundary Element Analysis of Plates and Shells (Beskos DE ed.). Springer-Verlag: Berlin, 1991, p. 93-140

[4] KRYSL, P., BELYTSCHKO, T.: *Analysis of thin shells by the element-free Galerkin method*, Int. J. Solids and Structures, 33, 1996, p. 3057-3080

[5] LU, P., A, M.: *Boundary element analysis of shallow shells involving shear deformation.* Int. J. Solids and Structures, 29, 1992, p. 1273-1282

[6] LUKASIEWICZ, S.: Local Loads in Plates and Shells, Noordhoff, London, 1979

[7] NEWTON, D.A., TOTTENHAM, H.: *Boundary value problems in thin shallow shells of arbitrary plan form*. Journal of Engineering Mathematics, 2, 1968, p. 211-223

[8] NOGUCHI, H., KAWASHIMA, T., MIYAMURA, T.: *Element free analyses of shell and spatial structures*, International Journal for Numerical Methods in Engineering, 47, 2000, p. 1215-1240

[9] PROVIDAKIS, C.P., BESKOS, D.: *Free and forced vibration of shallow shells by boundary and interior elements*, Computational Methods in Applied Mechanical Engineering, 92, 1991, p. 55-74

[10] REISSNER, E.: *Stresses and small displacements analysis of shallow shells*-II, Journal Math. Physics, 25, 1946, p. 279-300

[11] SLADEK, J., SLADEK, V., MANG, H.A.: *Meshless LBIE formulations for simply supported and clamped plates under dynamic load*. Computers and Structures, 81: 1643-1651. 2003

[12] SLADEK, J., SLADEK, V., WEN, P.H., ALIABADI, M.H.: *Meshless Local Petrov-Galerkin (MLPG) method for shear deformable shells analysis*. CMES: Computer Modeling in Engineering & Sciences, in print

[13] STEHFEST, H.: *Algorithm 368: numerical inversion of Laplace transform*. Comm. Assoc. Comput. Mach., 13, 1970, p. 47-49

[14] TOSAKA, H., MIYAKE, S.: *A boundary integral equation formulation for elastic shallow shell bending problems*. In Boundary Element Methods (Brebbia C.A., Futagami T. and Tanaka M. eds.), Springer, Berlin, 1983, p. 527-538

[15] WANG, J., SCHWEIZERHOF, K.: *Study on free vibration of moderately thick orthotropic laminated shallow shells by boundary-domain elements*, Applied Mathematical Modelling, 20, 1996, p. 579-584

[16] WANG, J., SCHWEIZERHOF, K.: *Boundary-domain element method for free vibration of moderately thick laminated orthotropic shallow shells*, Int. J. Solids and Structures, 33, 1996, p. 11-18

[17] ZHANG, J.D., ATLURI, S.N.: *A boundary/interior element method for quasi static and transient response analysis of shallow shells*, Computers and Structures, 24, 1986, p. 213-223